

A VISCOPLASTIC MODEL FOR THE FINITE STRAIN RESPONSE OF CRUSHABLE POLIMERIC FOAMS

Guilherme da Costa Machado, gcmachado@emc.ufsc.br

Marcelo Krajnc Alves, krajnc@emc.ufsc.br

Hilbeth Azikri Parente de Deus, hazikri@hotmail.com

Hazim Ali Al-Qureshi, hazim@emc.ufsc.br

Dep. Eng. Mecânica – Gmac, UFSC, CP 476, Florianópolis, SC, 88010-970, Brazil

Rodrigo Rossi, rossi@ucs.br

Dep. Eng. Mecânica – Gmac, UCS, Caxias do Sul, RS, 95070-560, Brazil

Abstract. *This paper proposes an elastoviscoplastic model for the finite deformation of crushable polymeric foams, which incorporates the phenomena of creep, relaxation and deformation rate sensitivity. Moreover, the model considers the deformation measure to be given by the logarithm or Henchy strain tensor, whose conjugate stress is the rotated Kirchhoff stress, and considers the elastic response to depend on the relative density of the material. The material is assumed to have a hardening behaviour which is characterized by two curves: one for the compaction response and one for the uniaxial compressive test. These hardening curves must be determined experimentally and introduced into the model. The evolution of the accumulated viscoplastic strain, which enables the determination of the viscoplastic multiplier, is based on a model that accounts for a saturation of the material response to the increase of the applied rate of deformation. The problem is formulated within a Total Lagrangian framework and is solved by the Galerkin finite element method. A set of simple problems is solved with the aim of attesting the proposed model and the robustness and performance of the algorithms employed in the discretization of the problem.*

Keywords *crushable foams, polymeric foams, finite visco-plasticity, finite element.*

1. INTRODUCTION

Polymeric foams are made of a skeleton composed of open or closed cells, which represent the basic unit of these materials. The mechanical response of polymeric foams depend on the cells geometric characteristics, such as cell wall thickness, shape and size distributions, and on the intrinsic properties of the polymer in the cell wall. In order to model such complex materials, different constitutive relations have been proposed in the literature and are basically divided into two groups: complex modeling approaches that proposes constitutive relation which describe the average behavior of the foam or simpler models that try to represent the cells as an assemblage of structural elements, see Gibson and Ashby (1997) and Landro *et al.* (2001).

In this work we consider a complex modeling approach and propose a hyperelastic-viscoplastic constitutive relation for modeling the behavior of open cell foam materials. Moreover, based on experimental results, we consider the hyperelastic response to depend on the relative density of the material. See Roberts and Garboczi (2001, 2002).

Among the various proposed constitutive relations, one can cite the power-law model, described in Chaboche and Rousselier (1983), that is generally accepted to give good predictions for low strain rates. However, as the strain rate increases, such a model is unable to describe the observed decreasing strain rate dependence. Also, in the limit, with the increase of the strain rate, the model should be capable to account for a saturation of the material response, as observed experimentally. With the aim of incorporating this material behavior in a unified viscoplastic model, other propositions for the flow rule have been used in the literature. Examples include a hyperbolic sine function, see Miller (1987), an exponential function or the addition of a second power-law function to the flow law, as proposed by Chaboche (1989, 1996). Some models even combine plasticity with viscoplasticity in order to achieve these goals, as seen in Almroth *et al.* (2004). Here, we make use of the constitutive equation proposed by Benallal, see Lemaitre (1996), which can be applied for large strain rates and account for the saturation of the overstress where the strain rate is very high.

The consideration of a viscoplastic model for the modeling of polymeric foams enables the incorporation of the following observed phenomena:

- Creep
- Relaxation
- Rate sensitivity

Creep phenomena is illustrated in Figure 1, in which Curve (abcd) represents the increase of the strain as a function of time as a result of a constant applied load. Also, Fig.1 shows that the creep response may be divided into 3 stages, given by:

1. Primary creeping, in which one observes a decreasing in the deformation rate due to the hardening of the material;
2. Secondary creeping: in which the strain rate is approximately constant, i.e., $\dot{\epsilon} \simeq \text{cte}$;

3. Tertiary creeping, in which one sees a fast increase in the deformation rate due to,
- A reduction of the transversal area,
 - The damage effect due to the nucleation, growth and coalescence of microvoids.

Figure 2 illustrates the influence of the stress-strain relation as a function of the applied strain rate. Also, it shows the existence of a linear elastic response of the material. However, in order to have an elastic response and recovery, one must have that $\dot{\epsilon} > 10^{-3} \text{ sec}^{-1}$. Such elastic response precludes the existence of a yield function. Now, it is important to observe that, if the temperature of the body is too elevated, the existence of a yield function may be questioned, since the material starts to behave more like a viscous fluid. In this work, we consider the temperature to be low and the deformation rate to be sufficiently high in order to consider the existence of an elastic response and a yield function.

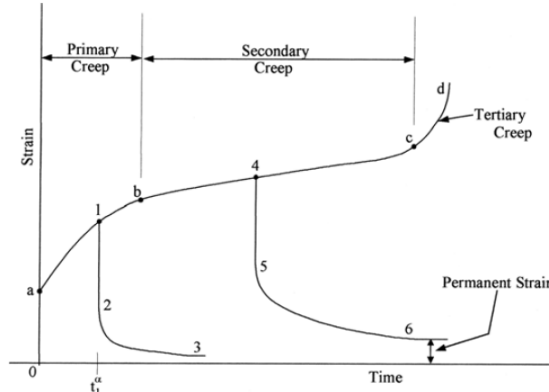
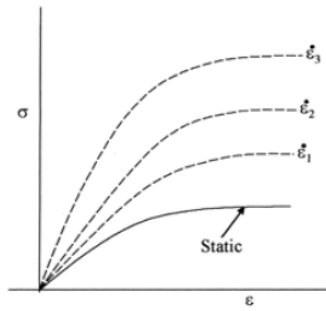


Figure 1 - Creep and relaxation tests



(a) Stress – strain behavior at different rates

Figure 2 – Rate of deformation sensitivity of the material response

2. THEORETICAL DEVELOPMENT

This paper proposes an elastoviscoplastic constitutive relation for the finite deformation of isotropic crushable polymeric foams, which incorporates the phenomena of creep, relaxation and deformation rate sensitivity in the response of the material. The model considers the material to have a hardening behavior that is characterized by two curves: one for the compaction response and one for the uniaxial compressive test, which must be determined experimentally. In addition, as a result of experimental observation, the model incorporates a different response in compression and tension and assumes the hyperelastic behavior to depend on the relative density of the material. In compression the ability of the material to deform volumetrically is enhanced by cell wall buckling processes as described by Gibson & Ashby (1997) and Girson *et al.* (1989). It is assumed that the foam cell deformation is not recoverable instantaneously and can be seen as being viscoplastic. Under tension loading, the cell walls break readily so the tensile load bearing capacity of crushable foams may be considerably smaller than its compressive load bearing capacity.

2.1. Multiplicative decomposition of the deformation gradient

Here, we assume the deformation gradient \mathbf{F} to be decomposed into an elastic deformation, \mathbf{F}^e , and a viscoplastic deformation, \mathbf{F}^{vp} as follows

$$\mathbf{F} = \mathbf{F}^e \mathbf{F}^{vp} \quad (1)$$

with

$$\mathbf{F} = \nabla_{\mathbf{x}} \varphi(\mathbf{X}, t), \quad (2)$$

in which $\mathbf{x} = \varphi(\mathbf{X}, t)$ denotes the deformation function. In addition, we define the deformation measure to be the logarithmic or Hencky strain tensor, given by $\mathbf{E}^e = \ln(\mathbf{U}^e)$, where $\mathbf{F}^e = \mathbf{R}^e \mathbf{U}^e$. Since the material is isotropic, the associated conjugate stress measure is given by the rotated Kirchhoff stress $\bar{\boldsymbol{\tau}}$, given by

$$\bar{\boldsymbol{\tau}} = (\mathbf{R}^e)^T \boldsymbol{\tau} (\mathbf{R}^e), \quad (3)$$

where $\boldsymbol{\tau}$ is the Kirchhoff stress, $\boldsymbol{\tau} = \det(\mathbf{F})\boldsymbol{\sigma}$, with $\boldsymbol{\sigma}$ denoting the Cauchy stress. See Peric and Owen (1998) and Weber and Anand (1990).

2.2. Definition of the yield surface

In order to define the yield function, we introduce the following basic definitions:

- The deviatoric rotated Kirchhoff stress, given by:

$$\bar{\boldsymbol{\tau}}^D = \bar{\boldsymbol{\tau}} - \frac{1}{3} \text{tr}(\bar{\boldsymbol{\tau}}) \mathbf{I} \quad (4)$$

- The von Mises effective rotated Kirchhoff stress, given by

$$q = \sqrt{\frac{3}{2} \bar{\boldsymbol{\tau}}^D : \bar{\boldsymbol{\tau}}^D} \quad (5)$$

- and the hydrostatic pressure stress, given by

$$p = -\frac{1}{3} \text{tr}(\bar{\boldsymbol{\tau}}). \quad (6)$$

Thus, from Eq. (4) and Eq.(6) we may express the rotated Kirchhoff stress as $\bar{\boldsymbol{\tau}} = \bar{\boldsymbol{\tau}}^D - p \mathbf{I}$.

Here, we consider the yield function for crushable foam materials, shown in Fig. 3, to be defined in terms of the Kirchhoff stress measure and given by

$$\mathcal{F}(q, p, \bar{\varepsilon}_k) = \sqrt{q^2 + \alpha(\bar{\varepsilon}_k)^2 (p - p_o(\bar{\varepsilon}_k))^2} - B(\bar{\varepsilon}_k), \quad (7)$$

in which $\alpha = \alpha(\bar{\varepsilon}_k)$ and $p_o = p_o(\bar{\varepsilon}_k)$ are functions of the internal variables $\bar{\varepsilon}_k$. The parameters p_o and B of the yield ellipse are related to the yield strength in hydrostatic compression, p_c , and to the yield strength in hydrostatic tension, p_t , by

$$p_o = 0.5(p_c - p_t), \quad B = \alpha A \quad \text{and} \quad A = 0.5(p_c + p_t), \quad (8)$$

where p_c and p_t are positive numbers and A is the length of the (horizontal) p -axis of the yield ellipse. The evolution of the yield ellipse is controlled by the volumetric compacting viscoplastic strain, $\bar{\varepsilon}_1 \equiv \varepsilon_v^p$, defined as

$$\varepsilon_v^p = -\ln(J^p), \quad \text{with} \quad J^p = \det(\mathbf{F}^p), \quad (9)$$

employed in the volumetric hardening model, and by the axial viscoplastic strain, $\bar{\varepsilon}_2 \equiv \varepsilon_a^p$, defined, in a unilateral compression test, as

$$\varepsilon_a^p = -\ln\left(\frac{L^p}{L_o}\right), \quad (10)$$

in which L^p is the unloaded length of the specimen, after the deformation has been applied, and L_o is the length of the initial configuration of the reference specimen.

To define the hardening behavior, some experimental test data must be obtained, which comprise:

- A uniaxial compression test data
- A hydrostatic compression test data

These hardening curves must be experimentally evaluated and incorporated to the model. Here, we assume the hydrostatic tension strength, p_t , to be proportional to the hydrostatic compression strength, i.e.,

$$p_t = \alpha_p p_c \quad (11)$$

for some constant value α_p , $\alpha_p \in [0.05, 0.10]$, see Hanssen *et al.* (2001) and Hallquist (1998). In addition, we assume the hydrostatic compression strength, p_c , to evolve as a result of compaction (increase in density) or dilation (reduction in density) of the material, i.e.

$$p_c = p_c^o + H_p(\bar{\varepsilon}_v^p) \quad (12)$$

where p_c^o is the initial hydrostatic compression yield strength and $H_p(\bar{\varepsilon}_v^p)$ is the hydrostatic compression strength hardening law, given in terms of the volumetric compacting viscoplastic strain.

In order to compute $\alpha = \alpha(\varepsilon_v^p, \varepsilon_a^p)$ a different independent experimental test is required. Here, we employ a uniaxial compression tests. Notice that, different tests could also have been considered. Now, since the type of impact loading that we want to simulate is dominated by a uniaxial compression type of loading, the best result for the analysis may be probably obtained by using a uniaxial compression test. From a uniaxial compression test we obtain

$$\bar{\tau}_y = \bar{\tau}_y^o + H(\bar{\varepsilon}_a^p) \quad (13)$$

where $\bar{\tau}_y^o$ is the initial yield stress, $H(\bar{\varepsilon}_a^p)$ is the strain hardening function and $\bar{\varepsilon}_a^p$ is the equivalent viscoplastic strain. Now in a general 3D case, the axial viscoplastic strain is not well defined. However, the uniaxial test response may be incorporated indirectly by using the uniaxial relation

$$\varepsilon_a^p = \frac{\varepsilon_v^p}{(1 - 2\nu_p)}. \quad (14)$$

Now, using (11-14), we can compute $\alpha = \alpha(\varepsilon_v^p, \varepsilon_a^p)$, as follows

$$\alpha = \frac{\bar{\tau}_y}{\left\{ p_t p_c - \frac{1}{3} \bar{\tau}_y (p_t - p_c) - \frac{1}{9} \bar{\tau}_y^2 \right\}^{\frac{1}{2}}}. \quad (15)$$

2.3. Visco plastic flow potential

The viscoplastic strain rate for the volumetric hardening model is assumed to be given by

$$\bar{D}^p = \dot{\lambda} \frac{\partial \mathcal{G}}{\partial \bar{\tau}}, \quad (16)$$

complemented by postulating a null viscoplastic spin, compatible with viscoplastic isotropy, i.e., $\bar{W}^p = 0$.

Here, $\dot{\lambda}$ is the viscoplastic multiplier which must satisfy: $\dot{\lambda} \geq 0$, which is given by a constitutive relation. The evolution of the viscoplastic deformation is computed as

$$\dot{\mathbf{F}}^p = \tilde{\mathbf{L}}^p \mathbf{F}^p \quad (17)$$

where

$$\tilde{\mathbf{L}}^p = (\mathbf{U}^e) \tilde{\mathbf{L}}^p (\mathbf{U}^e)^{-1}; \quad (18)$$

$$\bar{\mathbf{D}}^p = \frac{1}{2} (\tilde{\mathbf{L}}^p + [\tilde{\mathbf{L}}^p]^T); \quad (19)$$

and

$$\tilde{\mathbf{W}}^p = (\mathbf{U}^e)^{-1} \tilde{\mathbf{W}}^p (\mathbf{U}^e) = 0. \quad (20)$$

The viscoplastic flow potential for this model is given by

$$\mathcal{G}(q, p) = \sqrt{q^2 + \beta^2 p^2} \quad (21)$$

In which β is related to the plastic Poisson's ratio ν_p by

$$\beta = \frac{3}{\sqrt{2}} \sqrt{\frac{1-2\nu_p}{1+\nu_p}}. \quad (22)$$

The usual assumption, for polymeric foams is to consider $\nu_p = 0.0$. In the absence of the knowledge of the plastic Poisson's ratio, the consideration of a zero plastic Poisson's ratio is a reasonable assumption, as shown in Zhang *et al.* (1998), Gibson & Ashby (1997) and Gilchrist & Mills (2001).

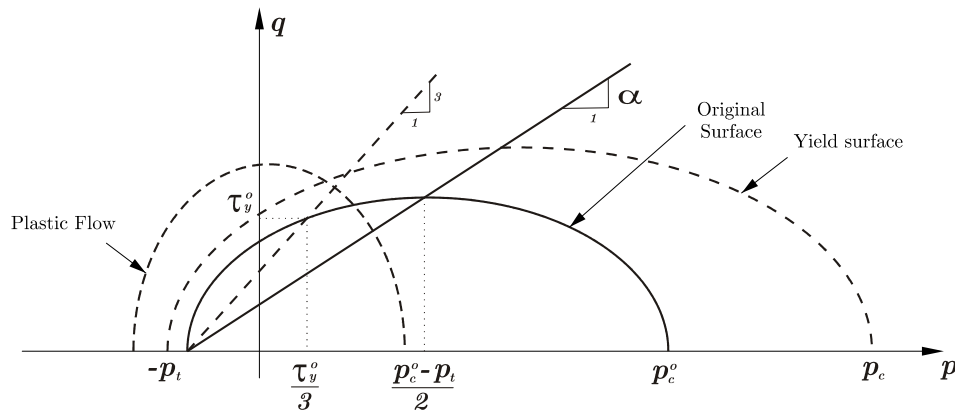


Figure 3 - Yield surface and flow potential on $p - q$ stress space.

2.4. Evolution law for the accumulated viscoplastic strain

In the case of viscoplastic materials, the viscoplastic multiplier λ is computed by solving a constitutive evolution equation. Here, we make use Benallal's model, see Lemaitre (1996), given by

$$\dot{\bar{\epsilon}}^p = \ln \left[\left(1 - \frac{\mathcal{F}(q, p, \bar{\epsilon}_v^p)}{K_\infty} \right)^{-M} \right] \quad (23)$$

where

$$\dot{\bar{\epsilon}}^p = \left\{ \frac{2}{3} \bar{\mathbf{D}}^p \cdot \bar{\mathbf{D}}^p \right\}^{\frac{1}{2}} \quad (24)$$

Notice that, the evolution of the accumulated viscoplastic strain, which enables the determination of the viscoplastic multiplier, is based on a model that accounts for a saturation of the material response to the increase of the applied rate of deformation. In fact, we have that

$$\mathcal{F}(q, p, \bar{\varepsilon}_k) = \sigma^v \geq 0 \quad (25)$$

where we denote σ^v as the over stress measure, we obtain

$$\sigma^v = K_\infty \left[1 - \exp\left(-\frac{\dot{\varepsilon}^p}{M}\right) \right]. \quad (26)$$

2.5. Hyperelastic response

Here, we consider the elastic response to be given, in terms of the logarithmic or Hencky strain tensor and the rotated Kirchhoff stress, as

$$\bar{\boldsymbol{\tau}} = \mathbb{D}(\rho^*) \mathbf{E}^e, \quad (27)$$

where

$$\mathbb{D}(\rho^*) = 2\mu(\rho^*) \mathbb{I} + \left(K(\rho^*) - \frac{2}{3}\mu(\rho^*) \right) (\mathbf{I} \otimes \mathbf{I}) \quad (28)$$

where $\mathbb{D}(\rho^*)$ is the fourth order elasticity tensor, \mathbb{I} is the fourth order identity tensor, \mathbf{I} is the second order identity tensor, $K(\rho^*)$ is the bulk modulus, $\mu(\rho^*)$ is the Lamé's coefficient or the shear modulus and ρ^* denoting the relative density, which is defined by the ratio of the foam density, ρ , with the fully compact material density, ρ_M , i.e.,

$$\rho^* = \frac{\rho}{\rho_M}. \quad (29)$$

The continuity equation may be written in terms of the relative density as

$$\rho_o^* = \det[\mathbf{F}] \rho^*, \quad (30)$$

in which $\rho_o^* = \rho_o^*(X)$ denotes the initial relative density, defined in the reference configuration, and $\rho^* = \rho^*(X, t)$ the actual relative density, defined at the reference configuration. Here, it's important to notice that the set of physical allowable relative densities, related to physical admissible deformation processes, is given by $\mathbf{K} = \{\rho^* \mid 0 < \rho^* \leq 1\}$.

In order to impose implicitly these constraints, we will rewrite the Young modulus as

$$E(\rho^*) = c(\rho^*)^\gamma E_M + I_K(\rho^*) \quad (31)$$

where $I_K(\rho^*)$ represents the indicator set of \mathbf{K} , i.e.,

$$I_K(\rho^*) = \begin{cases} 0, & \text{if } \rho^* \in \mathbf{K} \\ +\infty, & \text{if } \rho^* \notin \mathbf{K} \end{cases} \quad (32)$$

This expression may be regularized by using a combined internal and external penalty approaches, i.e., we consider a differentiable function $\Psi_\eta(\rho^*)$ such that

$$\lim_{\eta \rightarrow 0} \Psi_{\eta}(\rho^*) = I_K(\rho^*) \quad (33)$$

Given by

$$\Psi_{\eta}(\rho^*) = \bar{\eta} \frac{1}{\rho^*} + \frac{1}{\bar{\eta}} \left(\langle \rho^* - 1 \rangle^+ \right)^2 \quad (34)$$

Based on the above results, we consider the following constitutive relations

$$\nu(\rho^*) = \nu_M = \text{cte.} \quad (35)$$

and

$$E(\rho^*) = \left\{ c(\rho^*)^\gamma + \bar{\eta} \frac{1}{\rho^*} + \frac{1}{\bar{\eta}} \left(\langle \rho^* - 1 \rangle^+ \right)^2 \right\} E_M \quad (36)$$

with ν_M and E_M representing the Poisson's ratio and the Young's modulus of the fully dense material respectively and $\bar{\eta}$ a penalty parameter.

2.6. Incremental weak form of the problem

Let $\mathcal{K} = \{ \mathbf{u} \mid u_i \in W_s^1(\Omega), \mathbf{u} = \bar{\mathbf{u}} \text{ on } \Gamma_o^u \}$, for a sufficiently large s , denote the set of admissible displacements and $\mathcal{V} = \{ \delta \mathbf{u} \mid \delta u_i \in W_s^1(\Omega), \delta \mathbf{u} = \mathbf{0} \text{ on } \Gamma_o^u \}$ the set of admissible variations. The weak formulation of the problem may be stated as: Find $\mathbf{u}_{n+1} \in \mathcal{K}$ so that $F(\mathbf{u}_{n+1}; \delta \mathbf{u}) = 0 \quad \forall \delta \mathbf{u} \in \mathcal{V}$, i.e.,

$$F(\mathbf{u}_{n+1}^k; \delta \mathbf{u}) = \int_{\Omega} \mathbf{P}(\mathbf{u}_{n+1}^k) \cdot \nabla_x \delta \mathbf{u} \, d\Omega_o - \int_{\Omega} \rho_o \bar{\mathbf{b}}_{n+1} \cdot \delta \mathbf{u} \, d\Omega_o + \int_{\Gamma_o^t} \bar{\mathbf{t}}_{n+1} \cdot \delta \mathbf{u} \, dA_o \quad (37)$$

2.8. Numerical results

2.8.1. Uniaxial compression test

Here, the simulation of a uniaxial compression test is presented. The specimen consists of a cylindrical bar with a radius $R=28\text{mm}$ and a height of 50mm . The material parameters used in this analysis are described in Table 1. The process consists in prescribing the displacement of the upper part of the specimen, with a total upsetting of $\bar{u}_y = -32\text{mm}$, applied in order to compress the body. Due to the axisymmetry condition, only half of the domain is modeled. Figure 4 shows the displacement field, in the y-direction.

Table 1 – Material Parameters.

$E_m = 928,092 \text{ MPa}$	$\rho_o^* = 0,049$	$c = 0,30$
$\tau_y^o = 82,034 \text{ KPa}$	$\nu_p = 0,00$	$\eta = 0,00001$
$p_c^o = 40,470 \text{ KPa}$	$\nu = 0,25$	$M=4$
$\alpha=0,05$	$\gamma = 1,54$	$K_{\infty} = 20,0 \text{ KPa}$

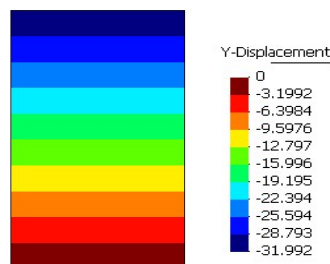


Figure 4 - Uniaxial compression test: Displacement field in the y-direction

Figure 5 shows the evolution of the volumetric plastic strain, associated with the homogeneous deformation process, as a function of the fraction, α_u , of the total applied upsetting. The total upsetting was applied incrementally, with constant increments, i.e., $u_y(\alpha_u) = \alpha_u * \bar{u}_y$.

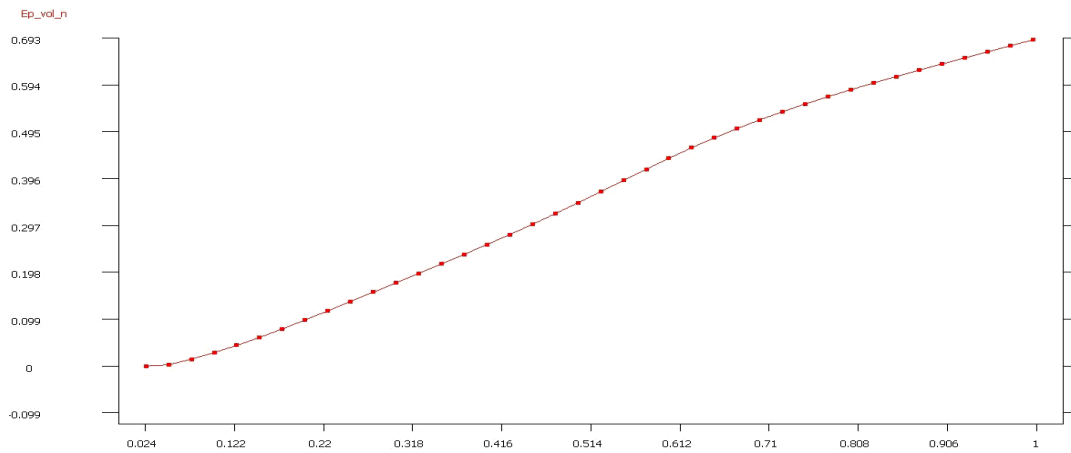


Figure 5 - Volumetric plastic strain versus α_u , fraction of the total applied upsetting.

Figure 6 shows the evolution of the relative density ρ^* as a function of α_u .

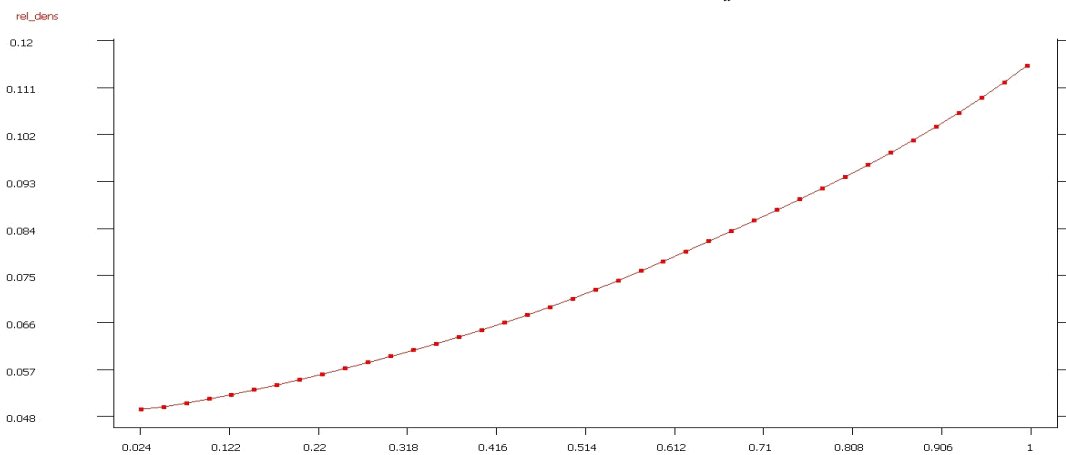


Figure 6 - Relative density versus fraction of the total applied upsetting

Figure 7 shows the evolution of the von Mises equivalent stress as a function of α_u .

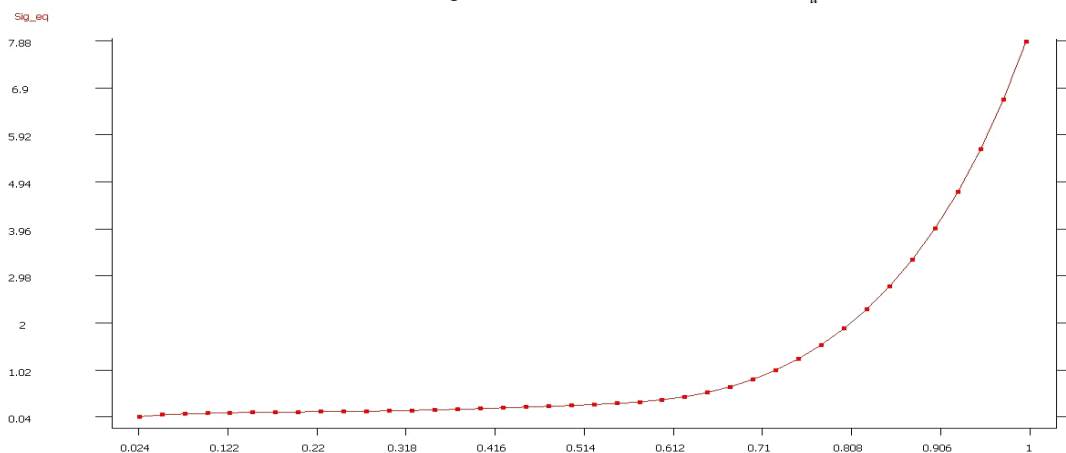


Figure 7 - von Mises stress (Cauchy) versus fraction of the applied upsetting

2.8.2. Conical slab

This example considers an axisymmetric problem that consists in the upsetting of a conical slab, whose dimensions are: $r_1=90mm$; $r_2=45mm$; $h=100mm$. The analysis consists in prescribing the displacement of the upper surface, with a total upsetting of $u_y=-51,25mm$, which was applied in 1000 step-increments, in an integration mesh with 240 Tri 6 elements. The parameters used in this analysis are the same presented in Table 1. Figure 8 depicts the level planes showing the displacement field, in the y-direction.

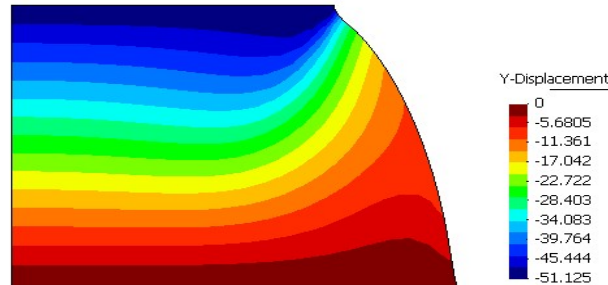


Figure 8 – Level planes representing the displacement field, in the y-component.

Figure 9 depicts level planes showing the distribution of the relative density of the foam material.

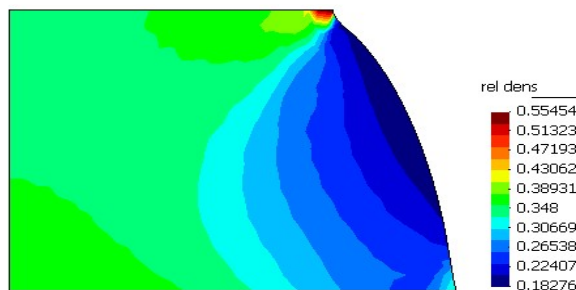


Figure 9 – distribution of the relative density field.

Figure 10 depicts level planes showing the distribution of the von Mises stress of the Cauchy Stress tensor.

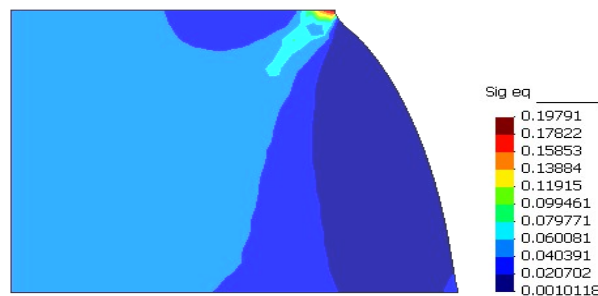


Figure 10 – distribution of the relative density field.

Figure 11 depicts level planes showing the distribution of the volumetric plastic strain measure, ϵ_v^p .

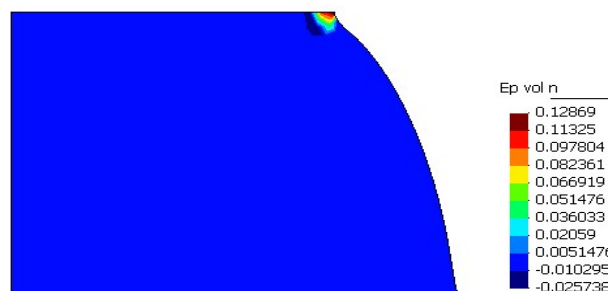


Figure 11 – Distribution of the volumetric plastic strain measure.

2.9. Discussion and conclusion

Polymeric foam constitutive behavior is extremely complex on the microstructural scale. Cellular buckling under compression initiates a long stress plateau. Further compression causes stress bottom up due to foam consolidation. Thus, adequate modeling of foam materials is still a challenge. Most of the problems are due to inadequate modeling of the elastic behavior of the material. The proposed model is able to represent some of the complex phenomena that occurs with crushable polymeric foams, which are: Creep, relaxation and rate sensitivity response. Moreover, the proposed model accounts for a saturation of the material response to the increase of the applied rate of deformation, as observed experimentally. Also, the paper addresses a complex problem that is the determination of non physical deformation processes, i.e., the determination of solutions that violates the model internal constraints. However, more testing is still necessary in order to verify the adequacy of the proposed model to simulate the deformation of real polymeric foam materials.

3. ACKNOWLEDGEMENTS

The support of the CNPq and Multibras S.A. is gratefully acknowledged.

4. REFERENCES

- Almroth P., Hasselqvist M., Simonsson K., Sjoström S., 2004, "Viscoplastic-plastic modelling of IN792", *Computational Materials Science* 29 (2004) 437–445.
- Chaboche J.L. and Rousselier G., 1983, "On the plastic and viscoplastic constitutive equations – part I: rules developed with internal variable concept", *Journal of Pressure Vessel Technology*, Vol. 105, pp. 153-158.
- Chaboche J.L., 1989, "Constitutive equations for cyclic plasticity and cyclic viscoplasticity", *Int. J. Plasticity*, Vol. 5, pp. 247-302.
- Chaboche J.L., 1996, "Unified cyclic viscoplasticity constitutive equations: development and thermodynamic framework", *Unified Constitutive Laws of Plastic Deformation*, Academic Press.
- Gibson L.J., Ashby M.F., 1997, "Cellular Solids: Structure and Properties", Cambridge University Press.
- Gilchrist A., Mills N.J., 2001, "Impact deformation of rigid polymeric foams: experiments and FEA modeling", *International Journal of Impact Engineering* Vol.25, pp. 767-786.
- Girson L.J., Ashby M.F., Zhang J. and Triantafillou T.C., 1989, "Failure Surfaces for Cellular Materials under Multiaxial Loads – I Modelling", *Int. J. Mech. Sci.*, Vol. 31, No. 9, pp. 635-663.
- Hallquist, J.O., 1998, "Theoretical Manual of LsDyna", Livermore Software Technology Corporation.
- Hanssen A.G., Hopperstad O.S., Langseth H., Ilstad H., 2001, "Validation of constitutive models applicable to aluminum foams", *International Journal of Mechanical Sciences*.
- Landro L., Sala G., Olivieri D., 2001, "Deformation mechanisms and energy absorption of polystyrene foams for protective helmets", *Polymer Testing* Vol.21, pp. 217-228.
- Lemaitre J. A., 1996, "A Course on Damage Mechanics", Springer, Berlin, Germany.
- Miller A.K., 1987, *Unified Constitutive Equations for Creep and Plasticity*, Elsevier applied Science
- Peric D., Owen D. R. J., 1998, "Finite-element applications to the nonlinear mechanics of solids", *Reports on Progress in Physics*, Vol. 61, pp. 1495-1574.
- Roberts, A.P., Garboczi E.J., 2002, "Elastic properties of model random three-dimensional open-cell solids", *Journal of the Mechanics and Physics of Solids*, Vol. 50, pp.33-55.
- Roberts, A.P., Garboczi E.J., 2001, "Elastic moduli of model random three-dimensional closed-cell cellular solids", *Acta Materialia*, Vol.49, pp.189–197.
- Weber G. and Anand, L., 1990, "Finite deformation constitutive equations and a time integration procedure for isotropic hyperelastic-viscoplastic solids", *Computer Methods in Applied Mechanics and Engineering*, Vol. 79, pp. 173-202.
- Zhang J., Lin Z., Wong A., Kikuchi N., Li V.C., Yee A.F, and Nusholtz G.S., 1997, "Constitutive Modeling and Material Characterization of Polymeric Foams", *Transactions of the ASME*, Vol. 119, pp.284-291.
- Zhang J., Kikuchi N., Li V.C., Yee A.F, and Nusholtz G.S., 1998, "Constitutive Modeling of Polymeric Foam Material Subjected to Dynamic Crash Loading", *Int. J. Impact Engng*, Vol. 21 No. 5 , pp.369-386.

5. RESPONSIBILITY NOTICE

The authors are the only responsible for the printed material included in this paper.